Environ. Sci. Technol. **2000**, *34,* 1529−1534

Cavitation Chemistry of Polychlorinated Biphenyls: Decomposition Mechanisms and Rates

GUANGMING ZHANG AND INEZ HUA*

School of Civil Engineering, Purdue University, West Lafayette, Indiana 47907-1284

Polychlorinated biphenyls (PCBs) are pollutants of environmental concern due to their widespread presence and persistence. The sonolytic destruction of aqueous polychlorinated biphenyls (PCBs) is reported in this article. The kinetics and transformation pathways were investigated at multiple frequencies and with various analytical tools. The pseudo-first-order rate constants for 2-PCB (4.6 μM), 4-PCB (5.4 μM), and 2,4,5-PCB (7.6×10^{-2} μM) were $2.1 \times 10^{-3} \pm 2.8 \times 10^{-5}$ s^{-1}, $1.6 \times 10^{-3} \pm 3.4 \times 10^{-5}$ s^{-1}, and $2.6 \times 10^{-3} \pm 9.4 \times 10^{-5}$ s^{-1}, respectively, when Ar-saturated solutions were sonicated at 20 kHz and an acoustic intensity of 30.8 W cm^{-2}. Chlorine recovery as chloride ion was 77%, 79%, and 70% for 2-PCB, 4-PCB, and 2,4,5-PCB under the same conditions. Electron spin resonance (ESR) experiments demonstrated that phenyl radical was formed during sonolysis of 2-PCB and 4-PCB. The formation of biphenyl, which was detected by mass spectroscopy, also indicates PCB dechlorination during sonication. Ethyl benzene, diethylbiphenyl, dibutylbiphenyl, phenol, propylphenol, and di-*tert*-butyl phenol were also detected by mass spectroscopy as products of PCB sonication. The kinetics of 2-PCB composition as well as the role of aqueous hydroxyl radical were examined at 20, 205, 358, 618, and 1071 kHz. The ultrasonic frequency significantly impacted the reaction rate and chloride recovery.

Introduction

Polychlorinated biphenyls (PCBs) are pollutants of major environmental concern due to their widespread presence, persistence, and implicated human carcinogenicity (*1, 2*). PCBs are distributed globally and are characterized by half-lives of several months in the atmosphere and 3−7 years in lakes (*2*). In 1979, the United States Environmental Protection Agency (U.S. EPA) banned production and distribution of PCBs, and as of 1981, approximately 6.3×10^8 kg of PCBs had been produced in the U.S. (*3*). An estimated 2.3×10^7 kg have been destroyed, and the remaining mass is distributed in landfills (1.4×10^8 kg), has been released into the environment (7.1×10^7 kg), or is still in use (3.9×10^8 kg) (*4*).

Numerous investigations have been carried out on the degradation of PCBs, although mechanistic information is limited (*3, 5*). At present there are no widely accepted methods for the large-scale remediation of water or soils contaminated with PCBs. Incineration of PCB contaminated soils or organic solvents requires high temperatures (950−1200 °C) and may form hazardous compounds such as dioxins (*2*). Biodegradation with microorganisms has been successful in laboratory studies but requires months for the transformation of highly chlorinated congeners to less substituted ones (*6*) and is limited by the ability of microorganisms to survive *in situ* (*1*). Chemical methods require additional reagents and lengthy treatment periods. PCB destruction by $Fe^{3+}/H_2O_2/UV$ (*5*), dechlorination with nanoscale Fe, and dechlorination on a Pd/Fe metal surface have been reported (*7, 8*). Fenton's reagent (*9*) and Y-ray destruction are also being investigated. Contaminated soils can be dealt with by washing the soil (surfactant washing) (*10*). However, further treatment of the residue is then necessary.

Sonication, a new technology, may be used to effectively destroy aqueous PCBs. The application of high power ultrasound to water results in a diverse range of chemical transformations and has been investigated for the destruction of environmental contaminants including *p*-nitrophenol (*11, 12*), carbon tetrachloride (*13*), pentachlorophenate (*14*), and oxygenated fuel additives such as methyl *tert*-butyl ether (*15*). Propagation of ultrasonic waves in water generates cavitation bubble clouds (*16*). Bubble implosion and fragmentation produce microregions of extreme conditions. Estimated temperatures within these microregions range from 2000 to 4000 K in aqueous solution (*17*). Thus, reaction pathways similar to those found in combustion occur during sonolysis (*18*). In addition to the direct high-temperature decomposition of organic solutes, water also undergoes thermolysis to release radical species (•H, •OH, HOO•) and hydrogen peroxide (H_2O_2) (*19, 20*). The concentration of •OH at the bubble-water interface has been estimated to be 4 mM (*21*). These free-radicals attack organic compounds present in solution and comprise another mechanism of sonochemistry.

We hypothesize that ultrasonic irradiation is an effective method for PCB destruction and that the transformation mechanism includes organic free-radicals. Furthermore, we hypothesize that varying the ultrasonic frequency affects reaction rates due to differential formation and transport of hydroxyl radical.

In this paper, we report the results of our investigation of the sonochemistry of aqueous PCBs. Our studies emphasized identification of reactive intermediates (organic free-radicals) and more stable byproducts of PCB destruction. Furthermore, we report the impact of ultrasonic frequency on PCB destruction kinetics and chloride ion recovery.

Materials and Methods

2-Chlorobiphenyl (2-PCB), 4-chlorobiphenyl (4-PCB), and 2,4,5-chlorobiphenyl (2,4,5-PCB) were purchased from Accustandard. Hexane was purchased from Fisher. *N-tert*-butyl-α-phenylnitrone (PBN) was purchased from Aldrich. All chemicals were used as received. Aqueous solutions were made with reagent grade water obtained from a Barnsted NANOpure ultrapure water system ($R = 18.3$ MΩ cm^{-1}).

Ultrasonic irradiation was performed with two ultrasonic systems. The first system was a high-intensity ultrasonic probe system (VCX-400 Sonics and Materials Inc.) which was operated at 20 kHz. The surface area of the probe was 1.32 cm^2, and the working volume of the stainless steel reactor was 165 mL. The acoustic power delivered into water was determined by the calorimetry method (*22*) to be 40.1 W. The second configuration (USW51 from AlliedSignal Inc.) was a multiple frequency system operating at 205, 358, 618, and 1071 kHz. The output power was 160 W, and the area of the emitting surface was 29 cm^2. The glass reactor used

* Corresponding author phone: (765)494-2409; fax: (765)496-1107; e-mail: hua@ce.ecn.purdue.edu.

10.1021/es981127f CCC: $19.00
Published on Web 03/07/2000

with this system had a volume of 400 mL. Both reactors were water-jacketed, and cooling water at 15 °C was used to control temperature during sonication.

Solutions of 2-PCB (5.2 or 4.6 μM) or 4-PCB (5.4 μM) were prepared by dissolving the compound in water and stirring for 1 week in a sealed volumetric flask. 2,4,5-PCB (7.6×10^{-2} μM) solutions were prepared by first dissolving the solid compound into hexane and then diluting the hexane solution. The concentration of hexane in final aqueous 2,4,5-PCB solution was 2×10^{-3} (v:v). During identification of the products by gas chromatography−mass spectroscopy (GC/MS), a higher concentration 2-PCB solution (54 μM) was prepared with 3×10^{-3} (v:v) methanol as a cosolvent. The spin-trap PBN (20 mM) was dissolved into the PCB solution just before sonication for ESR studies (*23*). No PBN was used in other experiments. Sodium carbonate (0.5, 5, 50, or 200 mM) was dissolved into PCB solutions for the free-radical scavenging experiments. The irradiated volume was continuously bubbled with Ar at 200 mL min^{-1}. During ESR experiments, Ar was passed through an Oxyclear O_2 trap (Labclear, Inc.) in order to remove trace amounts of O_2.

PCBs were quantified with a Hewlett-Packard 5890 gas chromatograph equipped with an electron capture detector (GC/ECD). Samples (5.0 mL) were withdrawn periodically from the reactor and extracted with 1.0 mL of hexane; the hexane extracts were injected into the GC (*24*). A DB5 column was used with the following temperature program: the initial temperature of 160 °C was held for 2 min, then increased at a rate of 5 °C/min to 210 °C, and maintained for 3 min. Standard solutions of PCBs in hexane were used for calibration of the instrument. Chloride ion was determined with a Dionex GP40 ion chromatograph equipped with an ASAI-4 column using an eluent comprised of 3.0 mM sodium carbonate and 2.7 mM sodium bicarbonate.

Identification of organic products was performed with a Finnigan MAT GVQ gas chromatograph−mass spectrometer (GC-MS) equipped with a DB1 column. The following temperature program was utilized: initial temperature held at 50 °C for 1 min, then increased to 280 °C at 10 °C/min, and maintained for 2 min. Free-radicals were detected with a Bruker ESP300 Electronic Spin Resonance Spectrometer (ESR) operating at 100 kHz, at a microwave power of 20 mW at 9.5 GHz. An aqueous sample (0.2 mL) was transferred to a quartz flat cell immediately after sonication, and the spectrum was acquired within 1 min of withdrawal from the ultrasonic reactor. A blank run, which consisted of sonicating only the dissolved spin-trap, was performed for each set of reactor conditions under which PCBs were sonicated. The ESR spectrum of the blank run was subtracted from the ESR spectrum of the PCB solution to produce the final spectrum.

Baseline runs without ultrasonic irradiation were carried out in order to examine the loss of PCBs via Ar sparging (200 mL min^{-1}) and adsorption to reactor walls. Both reactors were utilized: the glass reactor (multiple frequency system) and the stainless steel reactor (probe system). All other conditions were identical to those under which the actual sonication experiments were performed. The results showed that in the absence of sonication, PCB losses were insignificant (<3% in 1 h for both systems). The pH decreased from 7.5 to ~6.0 during sonication, which did not impact degradation of any of these congeners. All reported values are the average of multiple experimental results at each condition set.

Results and Discussion

The partitioning behavior of the congeners into different reactive regions within a cavitating solution is an important determinant of the pathway by which the congener reacts. Partitioning behavior is dependent upon the physicochemical characteristics of 2-PCB, 4-PCB, and 2,4,5-PCB, which are listed in Table 1. These congeners are highly hydrophobic and are expected to partition into the gas−liquid interface. Furthermore, the very low vapor pressures account for minimal loss during gas sparging.

TABLE 1. Physicochemical Properties of Selected PCBs[a]

congener	molecular weight (g mol^{-1})	log *P* (atm)	log *H* (L atm mol^{-1})	log K_{ow}	log *S* (mol L^{-1})
2-PCB	1.887×10^2	−4.66	-9.0×10^{-2}	4.53	−4.63
4-PCB	1.887×10^2	−5.33	-6.3×10^{-1}	4.40	−5.33
245-PCB	2.575×10^2	−6.95	-6.9×10^{-1}	5.78	−6.45

[a] *P*: vapor pressure *(42)*; *H*: Henry's constant; K_{ow}: octanol−water distribution constant; *S*: aqueous solubility *(43)*.

TABLE 2. Observed Rate Constants for Sonolytic PCB Destruction at 20 KHz

PCB congener	initial concn [μmol L^{-1}]	first-order rate constant [s^{-1}]	linear regression coefficient R^2
2-PCB	4.6	$2.1 \times 10^{-3} \pm 2.8 \times 10^{-5}$	9.8×10^{-1}
4-PCB	5.4	$1.6 \times 10^{-3} \pm 3.4 \times 10^{-5}$	9.6×10^{-1}
2,4,5-PCB	7.6×10^{-2}	$2.6 \times 10^{-3} \pm 9.4 \times 10^{-5}$	9.4×10^{-1}

We found that the sonolytic destruction of PCBs exhibits pseudo-first-order reaction kinetics at a given initial concentration (C_0) by performing a linear regression between $\ln(C/C_0)$ and sonication time, *t*. C = concentration of the PCB congener in each sample, and C_o = initial PCB concentration. Table 2 reports the rate constants of the three congeners sonicated at 20 kHz, 30.8 W cm^{-2}, and with an Ar sparge. Ninety-nine percent destruction of 2-PCB, 4-PCB, and 2,4,5-PCB occurs within 36, 47, and 29 min of sonication, respectively.

Cavitation chemistry encompasses complex pathways involving numerous reactive intermediates, and identification of these intermediates is crucial for elucidating the mechanism of sonochemistry. Free-radicals play an important role in the vapor phase chemistry of the bubble and also in aqueous reactions. For example, it has been reported that $\bullet CH_3$, $\bullet CH_2CH_2OH$, and $\bullet CH_2$-phenyl were produced during sonication of aqueous methanol, ethanol, and of pure toluene (*25*).

To identify organic free-radicals present at a significant concentration during the sonication of PCBs, we employed ESR with the aid of a spin trap, PBN. PBN reacts with the reactive free-radicals to form more stable spin-adducts, which are then detected by ESR (*26*). The ESR spectrum of a PBN spin adduct exhibits hyperfine coupling of the unpaired election with the ^{14}N and the β-H nuclei which leads to a triplet of doublets (*27*). The combination of the spin-adduct peak position and peak interval uniquely identifies the structure of a free-radical.

The first-derivative ESR spectra of 2-PCB and 4-PCB yielded interpretable signals, but no significant peaks were found when analyzing sonicated solutions of 2,4,5-PCB. The formation of organic radicals at a detectable level may have been hindered by the low aqueous solubility of 2,4,5-PCB.

Figure 1 is an ESR spectrum acquired after 10 min of sonicating an Ar-saturated solution of 2-PCB and PBN at 20 kHz. Samples that were irradiated at different power intensities for the same time period (10 min) are compared. Peaks consist of a triplet of doublets with the parameters of α_H = 4.2, α_N =16.0, which are characteristic α values for phenyl radical trapped by PBN (*28*). These peaks appeared in all ESR spectra obtained from sonicated solutions of 2-PCB (n = 20) and 4-PCB (n = 19) with irradiation times longer than 10 min (n = number of experiments).

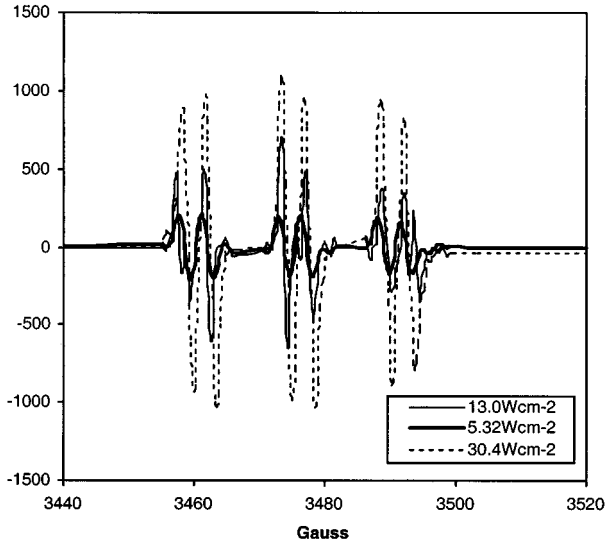

FIGURE 1. First-derivative ESR spectrum indicating the accumulation of PBN-phenyl after 10 min of sonicating an Ar-saturated solution of 2-PCB (4.6 μM) at 20 kHz and varying sound intensities.

Note that the integrated peak area (intensity) of the signal correlates with the spin adduct concentration and is therefore proportional to the initial concentration of free radical in solution (*29*). At the highest power intensity (30.4 W cm^{-2}), the peak intensity is highest. This indicates that the rate of formation of phenyl radical, and therefore, thermolytic cleavage of the biphenyl moiety, is accelerated at higher sound intensities. The enhancement can be understood by considering bubble implosion and the resulting conditions within the bubble. Acoustic intensity is directly related to acoustic pressure as described in eq 1 (*30*), which in turn determines the final temperatures and pressures within the bubble (eqs 2 and 3) (*31*).

$$I = \frac{P^2}{2\rho C} \tag{1}$$

$$T_{max} = T_o \frac{P_m(k-1)}{P_o} \tag{2}$$

$$P_{max} = P_o \left(\frac{P_m(k-1)}{P_o}\right)^{((k/k-1))} \tag{3}$$

where I = sound intensity, P = acoustic pressure, ρ = density of water, C = speed of sound in water. T_{max}, P_{max} = maximum temperature and pressure at implosion, T_0 = ambient temperature of water (22 °C in our experiments), P_0 = pressure in bubble at its maximum size (assumed to be the vapor pressure of water), P_m = peak pressure of the bubble, which is the sum of the hydrostatic and acoustic pressure (P, from eq 1), and k = polytropic index of saturating gas.

Thus, as the sound intensity increases, higher temperatures and pressures exist within the bubble interior, which then enhance the overall decomposition rate of the PCBs. In addition, the formation of organic free-radicals is also enhanced at higher sound intensities. These observations are consistent with previous reports of enhanced decomposition kinetics at higher acoustic intensities (*12*).

A second set of ESR experiments highlights the correlation between physicochemical properties and sonolytic decomposition kinetics. Figure 2 is a comparison of the first derivative spectra for separate, sonicated solutions of 2-PCB (4.6 μM) and 4-PCB (5.4 μM). Both congeners yield phenyl radical. Note that after 10 min of sonication at 30.4 W cm^{-2}, the signal intensity was higher for 2-PCB than for 4-PCB

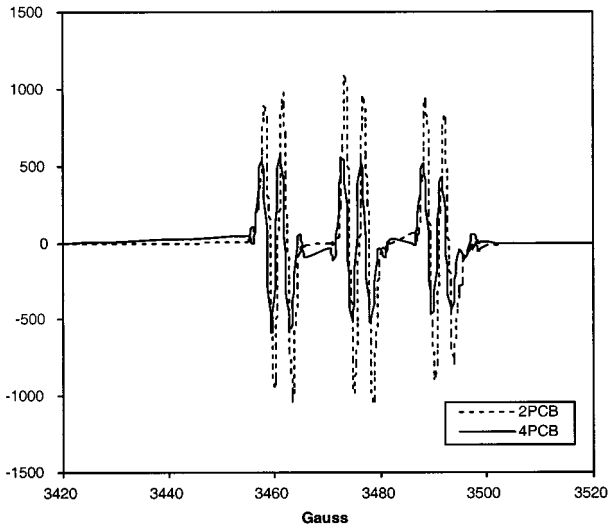

FIGURE 2. First-derivative ESR spectrum of PBN-phenyl detected after 10 min of sonicating separate solutions of 2-PCB (4.6 μM) or 4-PCB (5.2 μM) at 20 kHz and 30.4 W cm^{-2} in an Ar-saturated solution.

despite the lower initial concentration of 2-PCB. Because the mole ratio of spin-trap (20 mM) was in such large excess compared to either congener, the trapping efficiency was most likely the same for each congener. Also, formation of the phenyl radical involves thermolysis of C−C bond, which can only occur within high-temperature regions of the cavitation bubble (the bubble interior, or at the gas−liquid interface) and not within the bulk solution at ambient temperature. Therefore, a faster accumulation of phenyl radical is consistent with the hypothesis that a relatively greater number of 2-PCB (log $H = -0.09$) molecules partition into the bubble interior compared to 4-PCB (log $H = -0.63$) (Table 1).

Figure 3 demonstrates the time variation of the PBN-phenyl spin-adduct accumulation during sonication of 2-PCB. The spin-adduct initially accumulates, corresponding to formation of phenyl radical from the destruction of 2-PCB. Eventually, the intensity of the peak decreases because the concentration of the parent compound, 2-PCB, has decreased, and therefore, the rate of formation of phenyl radical decreases. Also, the spin-adduct itself further reacts during sonolysis. The formation of phenyl radical confirms thermolytic cleavage of the biphenyl rings, which is a key step in PCB destruction. Additional reactions yield other byproducts, which were identifiable by GC-MS.

Three groups of products were identified with the mass spectra of sonicated PCB solutions. The first group includes biphenyl and toluene, ethyl benzene, diethylbiphenyl, and dibutenylbiphenyl. The second group includes phenol, propylphenol, di-*tert*-butylphenol, and cyclohexenyl diphenol. Biphenyl was found only during the sonication of 54 μM 2-PCB, while others were detected as sonication products at lower initial concentration (5.2 μM) of 2-PCB. The third group consists of ethyl benzene, diethylbiphenyl, and trichlorophenol detected during the sonication of 2,4,5-PCB.

There are two possible pathways for formation of biphenyl. One is cleavage of C−Cl bond followed by H• addition:

$$C_{12}H_9Cl \rightarrow C_{12}H_9\bullet + Cl\bullet \tag{4}$$

$$C_{12}H_9\bullet + H\bullet \rightarrow C_{12}H_{10} \tag{5}$$

Another pathway is combination of two phenyl radicals:

$$C_{12}H_9Cl \rightarrow C_6H_5\bullet + C_6H_4Cl\bullet \tag{6}$$

$$C_6H_5\bullet + C_6H_5\bullet \rightarrow C_{12}H_{10} \tag{7}$$

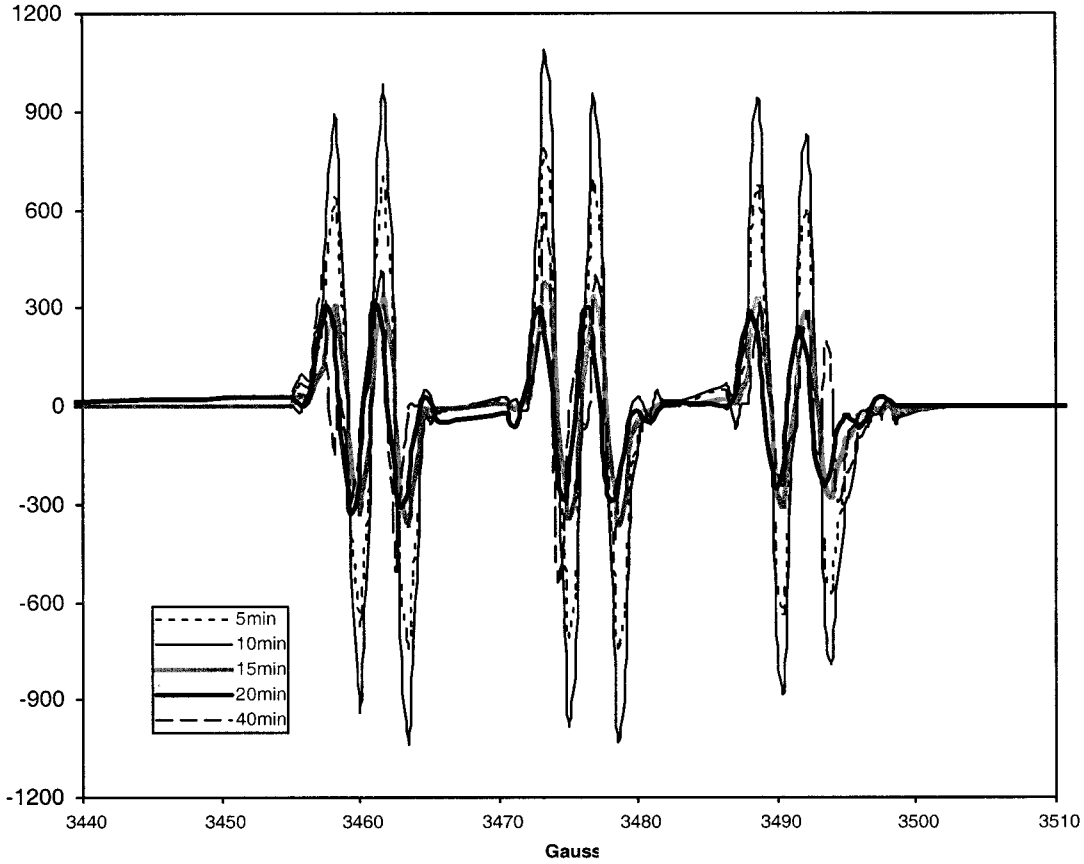

FIGURE 3. First-derivative ESR spectrum indicating the accumulation of PBN-phenyl during sonication of 2-PCB (4.6 μM) at 20 kHz and 30.4 W cm^{-2} in an Ar-saturated solution. A maximum peak area occurs after 10 min of sonication.

Bond energies can be used to estimate activation energies (*32*, *33*). Therefore, because the bond energy for Cl−$C_{12}H_9$ is lower (397 kJ mol^{-1}) than that of C_6H_5−C_6H_4Cl (418 kJ mol^{-1}), dechlorination is expected to occur more rapidly than recombination of the biphenyl. The ESR data cannot be used to differentiate between these two pathways, however, because Cl• is difficult to detect directly by ESR, due to its high reactivity (*34*). The following pathways are proposed for the formation of other compounds in the first group. The thermal degradation of phenyl radical can produce C_6H_4• (*35*):

$$C_6H_5\bullet \rightarrow C_6H_4\bullet + H\bullet \quad (8)$$

Alkyl fragments result from rupture of the aromatic ring. β-scission of phenyl radical will yield *n*-C_4H_3• and acetylene (*36*):

$$C_6H_5\bullet \rightarrow HC{\equiv}C{-}CH{=}CH{-}CH{=}CH\bullet \quad (9)$$

$$HC{\equiv}C{-}CH{=}CH{-}CH{=}CH\bullet \rightarrow HC{\equiv}C{-}CH{=}CH\bullet + C_2H_2 \quad (10)$$

The acetylene then reacts with OH• to form methyl radicals and carbon monoxide:

$$C_2H_2 + OH\bullet \rightarrow CH_3\bullet + CO \quad (11)$$

The formation of group one compounds results from reactions between the phenyl radical and C_6H_5•, C_6H_4•, C_4H_3•, CH_3•, H•, and C_2H_2. The presence of methanol as a cosolvent contributes to the formation of CH_3• and •CH_2OH during sonication of 54 μM 2-PCB but is unlikely to impact the formation of biphenyl. Group two compounds are formed by direct attack of group one compounds by •OH.

The third group of compounds (ethyl benzene, diethylbiphenyl, trichlorophenol) were detected during sonication of 2,4,5-PCB. Cleavage of the biphenyl ring yields a phenyl and a trichlorophenyl radical. Subsequent reaction of the phenyl radical with C_2H_2 will result in formation of ethyl benzene, and attack of the trichlorophenyl radical by •OH will yield trichlorophenol. The presence of hexane as a cosolvent can produce alkane free-radicals and may contribute to the formation of ethyl benzene and diethyl biphenyl. However, during sonication, C_2H_2 forms even in the absence of hexane. The wide range of organic byproducts detected by GC/MS results from the reaction of aromatic free-radicals with other carbon centered radicals or with hydroxyl radical (•OH). These experimental results confirm that free radical attack and thermolysis are major mechanisms in sonochemistry.

A major product of PCB sonication is chloride ion; PCBs are rapidly dechlorinated during sonolysis. Dehalogenation during sonication is desirable during the treatment of halogenated compounds for several reasons. Dechlorination to form inorganic chloride is advantageous because of the inert nature of chloride ion compared to other forms of chlorine. Production of inorganic chloride ion is therefore important for successful treatment of chlorinated pollutants. Also, highly substituted compounds tend to be difficult to transform microbially (*37*), and sonication may be a viable pretreatment.

The *chloride recovery ratio* was calculated as follows:

$$\text{chloride recovery ratio} = \frac{[Cl^-]}{([PCB]_i - [PCB]_f) \times n} \quad (12)$$

where $[Cl^-]$ = chloride ion concentration, mol L^{-1}, $[PCB]_i$ = initial PCB concentration concentration, mol L^{-1}, $[PCB]_f$ =

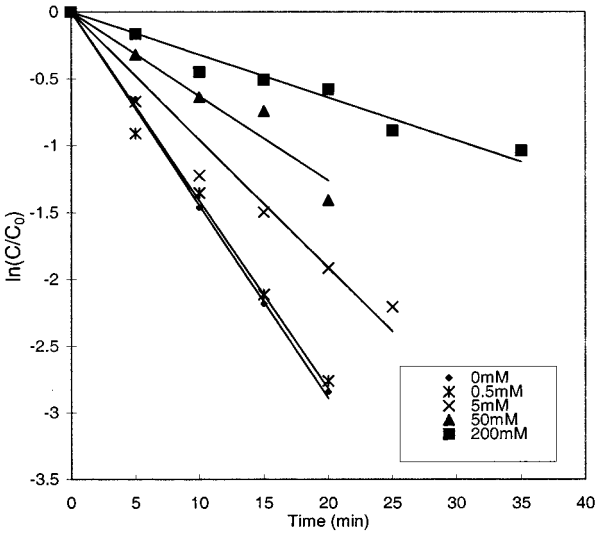

FIGURE 4. Inhibitory effect of carbonate on destruction of 2,4,5-PCB (7.6×10^{-2} μM) during sonolysis at 20 kHz and at 30.8 W cm^{-2} in Ar-saturated solutions. At carbonate concentrations of 0, 0.5, 5, 50, and 200 mM, the corresponding rate constants $k = 2.6 \times 10^{-3} \pm 9 \times 10^{-5}$ s^{-1}, $k = 2.4 \times 10^{-3} \pm 5.2 \times 10^{-5}$ s^{-1}, $1.5 \times 10^{-3} \pm 7.7 \times 10^{-5}$ s^{-1}, $1.2 \times 10^{-3} \pm 8 \times 10^{-5}$ s^{-1}, and $5 \times 10^{-4} \pm 5 \times 10^{-5}$s^{-1}.

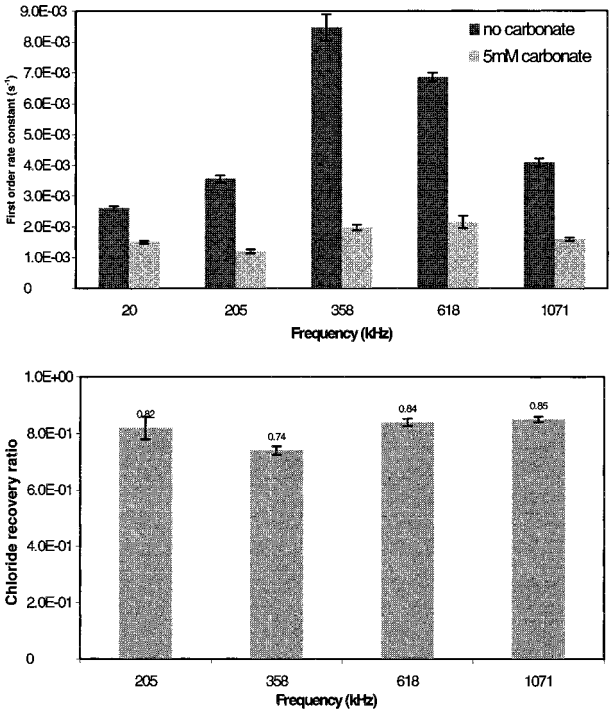

FIGURE 5. (a) (top): Observed rate constants for PCB destruction with and without carbonate. (b) (bottom): Chloride ion recovery at different frequencies. 2-PCB (5.2 μM) in an Ar-saturated solution, 5.5 W cm^{-2}.

final PCB concentration, mol L^{-1}, and n = number of chlorine atoms per congener.

When > 95% of the parent compound had been destroyed, the chloride recovery ratios were 77 ± 3%, 79 ± 4% and 70 ± 3% for 2-, 4-, and 2,4,5-PCB, respectively, at 20 kHz. The ratios were 82 ± 4% at 205 kHz, 74 ± 1.5% at 358 kHz, 84 ± 1.3% at 618 kHz, and 85 ± 1% at 1071 kHz for 2-PCB. Intermediate compounds formed during the decomposition of PCBs probably include volatile chlorinated organic compounds, which may vaporize during gas sparging, and account for the unrecovered chlorine.

As mentioned above, attack of free radical, especially •OH, is a major reaction pathway in sonochemistry. The attack of 2-PCB by •OH in water is very fast ($\sim 10^9$ L mol^{-1} s^{-1}), and substitution occurs at every possible position; seven hydro-2-PCB congeners were detected (*38*). To quantify the impact of •OH on PCB decomposition rate, Ar-saturated solutions consisting of 2,4,5-PCB and sodium carbonate were sonicated at 20 kHz ($I = 30.8$ W cm^{-2}). Carbonate is an effective •OH scavenger ($k = 3.9 \times 10^8$ L mol^{-1} s^{-1}) (*39*), and it does not undergo degradation during sonolysis. The high concentration of carbonate should trap virtually all of the aqueous phase •OH, preventing reaction with 2,4,5-PCB in the bulk solution. The pH remained higher than 10, and therefore the concentration of carbonate did not significantly change during the sonication.

The first-order plots of PCB destruction in the presence of 0 mM ($k = 2.6 \times 10^{-3} \pm 9 \times 10^{-5}$ s^{-1}), 0.5 mM ($k = 2.4 \times 10^{-3} \pm 5.2 \times 10^{-5}$ s^{-1}), 5 mM ($1.5 \times 10^{-3} \pm 7.7 \times 10^{-5}$ s^{-1}), 50 mM ($1.2 \times 10^{-3} \pm 8 \times 10^{-5}$ s^{-1}), and 200 mM ($5 \times 10^{-4} \pm 5 \times 10^{-5}$ s^{-1}) sodium carbonate are shown in Figure 4. Compared to sonication without carbonate, the scavenging of •OH by 200 mM carbonate decreases the rate constant by ~80%. •OH can react in the gas-phase or the bubble interface or diffuse into the bulk solution. Carbonate will only scavenge •OH at the bubble interface or in the bulk phase, and gas-phase reactions of •OH with PCBs will not be inhibited. Thus, the percentage reduction in the reaction rate indicates only the relative significance of •OH attack in the liquid phases. The differential role of •OH attack over a range of ultrasonic frequencies was also investigated with a series of scavenger experiments.

Ar-saturated solutions of 2-PCB were sonicated at 205, 358, 618, 1071 kHz, in the presence and in the absence of a scavenger (5 mM sodium carbonate). In the absence of carbonate, the rate constants were $3.6 \times 10^{-3} \pm 7.8 \times 10^{-5}$ s^{-1}, $8.5 \times 10^{-3} \pm 4.2 \times 10^{-5}$ s^{-1}, $6.9 \times 10^{-3} \pm 1.4 \times 10^{-5}$ s^{-1}, and $4.1 \times 10^{-3} \pm 1.2 \times 10^{-5}$ s^{-1} (Figure 5a). The rate constant at 20 kHz without carbonate can be found in Table 2. Sonication at 358 kHz exhibits the fastest kinetics. However, the chloride ion recovery ratio is lowest at 358 kHz (Figure 5b). Chloride ion results primarily from thermolytic cleavage of C−Cl bond, while PCB transformation is a result of thermolysis and free radical attack. Therefore, we propose that free radical attack (especially •OH) in the aqueous phase plays a more significant role at 358 kHz than at the other three frequencies. To test the hypothesis, we employed 5 mM sodium carbonate to scavenge •OH and examined the decline in PCB destruction rate (Figure 5a). The rate constants were $1.2 \times 10^{-3} \pm 6.1 \times 10^{-5}$, $2.0 \times 10^{-3} \pm 9.1 \times 10^{-5}$, $2.2 \times 10^{-3} \pm 2.0 \times 10^{-4}$, and $1.6 \times 10^{-3} \pm 6.0 \times 10^{-5}$ s^{-1} for 205, 358, 618, and 1071 kHz, respectively. At 20 kHz, $k = 1.2 \times 10^{-3} \pm 4.1 \times 10^{-5}$ s^{-1}. Clearly, carbonate inhibits 2-PCB degradation at any frequency but most significantly at 358 kHz. Note also that at the same carbonate concentration (5 mM), the impact was less at 20 kHz than at higher frequencies.

During sonication, PCBs in the bulk liquid phase transform primarily by reaction with •OH. The attack of solutes by •OH occurs only after the radicals reach the interface and/or the bulk solution (*40*), where the carbonate scavenges •OH. Destructive mechanisms which occur within the cavitation bubble (e.g., thermolysis) will not be inhibited by the presence of carbonate. Therefore, from our data, we conclude •OH attack contributes substantially to the enhanced sonochemical decomposition rates at 358 kHz.

A number of factors determine the observed rate constant in an ultrasonic reactor, and ultrasonic frequency clearly impacts the rate of PCB destruction during sonolysis. However, the mechanism by which ultrasonic frequency enhances reaction rates has not been definitively reported.

There are indications that the conditions within the bubble interior vary with frequency, based upon sonoluminescence studies (*41*). Other investigators hypothesize that the flux of hydroxyl radicals is enhanced based on changes in the bubble hydrodynamics during sonolysis (*40*).

In summary, aqueous PCBs rapidly decompose when exposed to ultrasound. Both thermolysis and free radical attack are important pathways of PCB destruction. Our conclusions are based upon monitoring the concentration of the parent compounds, identifying and measuring the formation of phenyl radical, and characterizing organic byproducts during sonolysis. Furthermore, we compare chloride ion recoveries and PCB destruction kinetics over a range of ultrasonic frequencies. Ultrasonic irradiation is optimal at 358 kHz, but the chloride recovery is optimal at 1071 kHz. The differential role of aqueous •OH attack was confirmed over a range of ultrasonic frequencies.

Acknowledgments

The authors wish to thank the United States Department of Energy (DOE Grant Number DE-FG07-96ER14710) and the Purdue Research Foundation (Award Number 6902644) for funding these studies. We also thank Dr. Carl Wood and Connie Bonham at the Mass Spectrometry Service Center of Purdue University for analysis of mass spectra and Dr. Michael Everly of The Jonathan W. Amy Facility for Chemical Instrumentation (JAFCI) at Purdue University for help with the ESR experiments.

Literature Cited

(1) Bumpus, J. A.; Tien, M.; Wright, D.; Aust, S. D. *Science* **1985**, *228*, 1434−1436.
(2) *PCBs and the Environment*; Waid, J. S., Ed.; CRC Press: Boca Raton, FL, 1986.
(3) Morris, S.; Lester, J. N.. *Water Res.* **1994**, *28*, 1553−1561.
(4) May, H. D. *Appl. Environ. Microbiol.* **1992**, *58*, 3088.
(5) Pignatello, J. J.; Chapa, G. *Environ. Toxicol. Chem.* **1994**, *13*, 423−427.
(6) Dort, H. M.; Smullen, L. A.; May, R. J.; Bedard, D. L. *Environ. Sci. Technol.* **1997**, *31*, 3300−3307.
(7) Wang, C.; Zhang, W. *Environ. Sci. Technol.* **1997**, *31*, 2154−2156.
(8) Grittini, C.; Malcomson, M.; Fernando, Q.; Korte, N. *Environ. Sci. Technol.* **1995**, *29*, 2898−2900.
(9) Sedlak, D. L.; Andren, A. W. *Environ. Sci. Technol.* **1991**, *25*, 1419−1427.
(10) Abdul, A. S.; Ang, C. C. *Ground Water* **1994**, *32*, 727−734.
(11) Weavers, L. K.; ling, F. H.; Hoffmann, M. R. *Environ. Sci. Technol.* **1998**, *32*, 2727−2734.
(12) Hua, I.; Hochemer, R. H.; Hoffmann, M. R. *Environ. Sci. Technol.* **1995**, *29*, 2790−2796.
(13) Hua, I.; Hoffmann, M. R. *Environ. Sci. Technol.* **1996**, *30*, 864−871.
(14) Petrier, C.; Micolle, M.; Merlin, G.; Luche, J.; Reverdy, G. *Environ. Sci. Technol.* **1992**, *26*, 1639−1642.
(15) Kang, J.; Hoffmann, M. R. *Environ. Sci. Technol.* **1998**, *32*, 3194−3199.
(16) Bhatnagar, A.; Cheung, H. M. *Environ. Sci. Technol.* **1994**, *28*, 1481−1486.
(17) Misik, V.; Miyoshi, N.; Riesz, P. *J. Phys. Chem.* **1995**, *99*, 3605−3611.
(18) Henglein, A. *Ultrasonics* **1987**, *25*, 6.
(19) Hart, E. J.; Henglein, A. *J. Phys. Chem.* **1987**, *91*, 3654−3656.
(20) Hua, I.; Hoffmann, M. R. *Environ. Sci. Technol.* **1997**, *31*, 2237−2243.
(21) Gutierrez, M.; A, A. H. *J. Phys. Chem.* **1991**, *95*, 6044−6047.
(22) Henglein, A.; Gutierrez, M. *J. Phys. Chem.* **1990**, *94*, 5169.
(23) Davis, M.; Slater, T. F. *Chem. Bio. Interactions* **1986**, *58*, 137−147.
(24) Wells, D. E. *Environmental analysis: techniques, applicaitons and quality assurance*; Elsevier Science Publishers: 1993.
(25) Misik, V.; Riesz, P. *Ultrasonics Sonochemistry* **1996**, *3*, S173−S186.
(26) Kondo, T.; Riesz, P. *Free Radical Biol. Med.* **1989**, *7*, 259−268.
(27) Rehorek, D.; Henning, H.; Dubose, C. M.; Kemp, T. J.; Janzen, E. G. *Free Rad. Res. Comms.* **1990**, *10*, 75−84.
(28) Hill, H. A. O.; Thornalley, *Biochim. Biophys. Acta* **1983**, *762*, 44−51.
(29) Sargent, F. P.; Gardy, E. M. *Can. J. Chem.* **1976**, *54*, 275−279.
(30) Glickstein, C. *Basic Ultrasonics*; John Rider Publisher: 1960.
(31) Noltingk, B. E.; Neppiras, E. A. *Proc. Phys. Soc. B* **1950**, *63B*, 674.
(32) Atkins, P. W. *Physical Chemistry*, 3rd ed.; W. H. Freeman Com: New York, 1984; p 857.
(33) Brezonik, P. L. *Chemical kinetics and process dynamics in aquatic systems*; Lewis Publishers: Boca Raton, 1993; p 754.
(34) Janzen, E. G. *Anal. Chem.* **1974**, *46*, 478R−490R.
(35) Kern, R. D.; Xie, K.; Chen, H. *Combust. Sci. Technol.* **1992**, *85*, 77−82.
(36) Sethuraman, S.; Senka, D. M.; Gutma, D. *Combust. Sci. Technol.* **1992**, *82*, 13−30.
(37) Bedard, D. L.; Quensen, J. F. *Microbial transformaiton and degradation of toxic organic chemicals*; Wiley-Liss Inc.: 1995.
(38) Sedlak, D. L.; Andren, A. W. *Environ. Sci. Technol.* **1991**, *25*, 777−782.
(39) Buxton, B. *J. Phys. Chem. Ref. Data* **1988**, *17*, 516.
(40) Petrier, C.; Jeunet, A.; Luche, J.; Reverdy, G. *J. Am. Chem. Soc.* **1992**, *114*, 3148−3150.
(41) Didenko, Y. T.; Nastich, D. N.; Pugach, S. P.; Polovinka, Y. A.; Kvochka, V. I. *Ultrasonics* **1994**, *32*, 71−76.
(42) Schwarzenbach, R. P.; Gschwend, P. M.; imboden, D. M. *Environmental organic chemistry*; John Wiley & Sons Inc.: 1993.
(43) Nirmalakhandan, N. N.; Speece, R. E. *Environ. Sci. Technol.* **1989**, *23*, 708−713.

Received for review November 2, 1998. Revised manuscript received May 11, 1999. Accepted November 2, 1999.

ES981127F